Investigation of a Full-Scale Wide Chord Blade Rotor System in the NASA Ames 40- by 80-Foot Wind Tunnel

Patrick M. Shinoda
Army/NASA Rotorcraft Division
Aeroflightdynamics Directorate (AMRDEC)
U.S. Army Research, Development, and Engineering Command
Ames Research Center
Moffett Field, California
pshinoda@mail.arc.nasa.gov

Thomas R. Norman and Stephen A. Jacklin
Army/NASA Rotorcraft Division
NASA Ames Research Center
Moffett Field, California
tnorman@mail.arc.nasa.gov and
sjacklin@mail.arc.nasa.gov

Hyeonsoo Yeo
Raytheon ITSS
NASA Ames Research Center
Moffett Field, California
hsyeo@mail.arc.nasa.gov

Andreas P.F. Bernhard
Sikorsky Aircraft Corporation
Stratford, Connecticut
ABernhard@SIKORSKY.COM

Axel Haber
ZF Luftfahrttechnik GmbH
Kassel-Calden, Germany
axel.haber@zf.com

ABTRACT

A full-scale four-bladed UH-60/Wide Chord Blade rotor system was tested in the NASA Ames 40- by 80-Foot Wind Tunnel. A quality data set at forward speeds of 60 to 150 knots were obtained to support future rotor developments and analysis improvements. The rotor performance data were compared with flight test data and CAMRAD II predictions. Wind tunnel comparisons with flight test data show good agreement at all advance ratios tested except above an advance ratio of 0.30. CAMRAD II power calculations show good agreement with full-scale wind tunnel data at advance ratios between 0.20 to 0.35 and poor agreement at advance ratio of 0.15. CAMRAD II propulsive force calculations show fair to good correlation with full-scale wind tunnel data at all advance ratios tested.

NOTATION

A = rotor disk area, πR^2, ft^2

A_{TS} = test section area, ft^2

c.g. = center of gravity

C_{LR} = rotor wind-axis lift coefficient, positive up, $L_R/A\rho(\Omega R)^2$

C_P = main rotor power coefficient, $P/A\rho(\Omega R)^3$

$C_{P\ Total}$ = total rotor power coefficient, $P/A\rho(\Omega R)^3$

$\bar{C}_P$ = main rotor power coefficient, normalized

$\bar{C}_{P\ Total}$ = total rotor power coefficient, normalized

C_T = rotor thrust coefficient, positive up, $T/A\rho(\Omega R)^2$

C_{XR} = rotor wind-axis propulsive coefficient, positive forward, $-D_R/A\rho(\Omega R)^2$

$\bar{C}_{XR}$ = rotor wind-axis propulsive coefficient, normalized

C_W = weight coefficient, positive up $GW/A\rho(\Omega R)^2$

D_R = rotor wind-axis drag, positive downstream, lb

GW = aircraft gross weight, lb

L_R = rotor wind-axis lift, positive up, lb

P = rotor shaft power, Torque * Ω, ft-lb/s

P_{Total} = total engine power, Torque * Ω, ft-lb/s

q = free stream dynamic pressure, lb/ft^2

R = rotor radius, ft

Presented at the American Helicopter Society 4th Decennial Specialist's Conference on Aeromechanics, San Francisco, CA, January 21-23, 2004.

T = rotor thrust, lb

V_∞ = free stream velocity, ft/s

α_c = corrected angle of attack, deg

$\Delta\alpha$ = induced angle correction, deg

α_s = rotor shaft angle, positive aft of vertical, deg

δ_W = boundary correction factor

μ = advance ratio, $V_\infty/\Omega R$

ρ = free-stream air density, slug/ft^3

Ω = rotor rotational speed, rad/s

INTRODUCTION

Wind tunnel testing has been extensively used in the development and improvement of rotorcraft designs in addition to providing databases for refinement of theoretical models. It is also important to compare and assess these results with helicopter flight test data.

Sikorsky Aircraft Corporation conducted two flight test programs to evaluate the performance and dynamic characteristics of the wide chord blade design. In the first flight test, a standard UH-60A rotor and a number of different wide chord blade rotors were evaluated on a UH-60L aircraft. The second flight test had the production wide chord blade design which was called the Growth Rotor Blade (GRB) on both the UH-60L and MH-60K helicopters.

To expand the existing wide chord blade (WCB) database and to investigate rotor performance and loads in the midrange to cruise flight regime, a full-scale WCB rotor test was conducted in the NASA Ames 40- by 80-Foot Wind Tunnel (40 x 80). In this paper, the results from this test program are compared with flight test and with predictions to 1) assess the flight test data, 2) evaluate wind tunnel test data with flight test data, and 3) evaluate and validate analytical modeling capabilities in the 60-150 knot speed range.

This paper presents a brief description of the current wind tunnel test, the analytical model used, and the two flight tests using various wide chord rotor sets. Wind tunnel forward flight rotor performance results are discussed and compared with flight test data, and analytical calculations. Finally, conclusions of the research are presented.

DESCRIPTION OF THE TEST

The following section provides a brief description of the test, including the test stand, rotor system, the test stand primary measurement system, test conditions, and wall corrections. A more detailed description of the test stand model and standard measurement system can be found in Ref. 1.

Test Stand

The test program was conducted in the NASA Ames 40- by 80-Foot Wind Tunnel using a set of Sikorsky Aircraft wide chord blades installed on a production Sikorsky UH-60 rotor hub system that was mounted on NASA's Large Rotor Test Apparatus (LRTA). Figure 1 shows the model installed in the wind tunnel.

The LRTA test stand (Fig. 2) was designed for testing large-scale helicopter rotors and tilt rotors in the NASA Ames National Full-Scale Aerodynamics Complex. The test stand houses two electric drive motors, a transmission, rotor balance, self-contained lubrication system, and a primary and dynamic control system. The LRTA is capable of testing rotors up to 52,000 lb thrust and 6,000 HP and can measure six-components of both steady and dynamic rotor hub loads. The primary controls consist of three electrical-mechanical actuators that provide conventional collective and cyclic pitch control. A hydraulic-based dynamic control system is integrated into the primary control system and can excite the non-rotating swashplate from 0 to approximately 25 Hz. The LRTA fairing (a symmetrical body of revolution 40-ft in length and 8.33-ft in diameter) is mounted independently of the LRTA chassis frame on load cells and provides fuselage forces (lift, drag, side force) and moments (pitch, roll, yaw).

The LRTA was mounted in the wind tunnel on a three-strut (two main struts and one tail strut) support system placing the rotor hub nominally 20.4-ft above the wind tunnel floor. The test stand angle-of-attack was varied by changing the height of the gimballed tail strut.

Rotor System

The rotor system components, including the hub, spindles, and swashplate, are production UH-60 components. The four-bladed, articulated rotor system consists of four subsystems: hub, blade pitch controls, bifilar vibration absorber, and main rotor blades. The four main rotor blades attached to spindles are retained in a one-piece titanium hub by elastomeric bearings. These bearings permit the blade to pitch, flap, and lead-lag. Main rotor dampers are installed between each of the main rotor spindles and the hub to restrain lead and lag motions of the main rotor blades during rotation and to absorb rotor head starting loads. Blade pitch is controlled through adjustable pitch links that are moved by the swashplate. The bifilar vibration absorber is designed to reduce rotor vibration at the rotor head. The absorber is mounted on top of the hub and consists of a four-arm plate

with attached weights. For this test program, the bifilar weights were not installed.

The wide chord blades (WCB) used in this test were previously flight tested on a UH-60L aircraft. The blades had an all-composite graphite/glass-tubular spar with an increased chord (10% increase in solidity), advanced airfoils (SC2110 and SSCA09), and a swept-tapered tip with anhedral. Six configurations or variants of the wide chord blade were tested in the first flight test program. The differences between these configurations were mostly in the mid-span and leading edge tip weights; the blade geometry and aerodynamic characteristics are the same. The production configuration was tested during the second flight test program. One of the configuration blade sets from the first flight test program was tested in the 40 x 80 wind tunnel. The differences between the standard UH-60 rotor blade and the wide chord blade planforms are shown in Fig. 3 and described in Table 1.

Primary Measurements

The performance measurements discussed in this paper were obtained from the LRTA five-component balance and flex coupling. The balance measures rotor normal, axial and side forces, together with the rotor pitching and rolling moments. The instrumented flex coupling measures rotor torque and residual power-train normal force. Both rotor balance and flex coupling were designed to measure static and dynamic loads. For this program, however, the measurement systems were only calibrated statically. Table 2 lists the general balance capabilities and Table 3 the accuracy of the system. Detailed information on the balance, including calibration procedures, can be found in Ref. 2.

Test Conditions

Performance data were acquired in forward flight over a range of thrust, speed, and shaft angles by performing thrust sweeps at specific tunnel velocities and rotor shaft angles-of-attack. The full range of test conditions is listed in Table 4. All data presented in this paper were acquired with the first harmonic flapping trimmed to near zero (± 0.4 deg) and have wall corrections applied.

Wall Corrections

The wall corrections applied to the rotor performance data are based on Glauert's methodology (Ref. 3) for fixed wing testing in a wind tunnel. The induced angle correction or downwash, as used in the 40- by 80-Foot Wind Tunnel, is

$$\Delta\alpha = \frac{180}{\pi}\delta_W \frac{L}{qA_{TS}} \qquad \text{[deg]} \qquad (1)$$

where L is the rotor lift, A_{TS} is the test section area, q is the tunnel dynamic pressure and δ_W is the boundary correction factor. The boundary correction factor, δ_W, is dependent on the test section shape, the ratio of the wing span or rotor diameter to tunnel width and the position of the wing or rotor in the test section. The boundary correction factor (δ_W = 0.091) for the 40- by 80-Foot Wind Tunnel was determined from Ref. 4, Fig. 7. The resultant corrected angle of attack is

$$\alpha_C = \alpha_S + \Delta\alpha \qquad \text{[deg]} \qquad (2)$$

where α_S is the rotor shaft angle and $\Delta\alpha$ is the induced angle correction. The wind tunnel wall correction, in the form of the induced angle correction, is used to correct the 40 x 80 rotor lift and rotor propulsive force at the various physical rotor shaft angles, thrust, and advance ratios; no direct wall correction is applied to power. This correction was applied to all the wind tunnel data presented in this paper.

DESCRIPTION OF FLIGHT TESTS

Rotor performance data from two flight test programs are presented in this paper. This section provides a summary of these tests.

The first flight test program was a joint Sikorsky/Army feasibility test program conducted from November 1993 through October 1995. Both standard and wide chord blades were tested on aircraft 84-23953, which is a UH-60A upgraded to a UH-60L for test purposes. These upgrades were mainly internal to the aircraft: upgraded engines, improved gearbox, tail rigging changes and flight control modifications.

The second flight test program was a joint Sikorsky/Army follow-on program to the feasibility test program discussed previously. In this program, the production wide chord blade or Growth Rotor Blade (GRB) was being qualified for the UH-60L and MH-60K helicopters. Flight tests were conducted from March 1999 to November 1999. Level flight data from both flight tests are used to compare with the 40 x 80 wind tunnel data in this paper.

DESCRIPTION OF ANALYTICAL MODEL

Isolated Rotor Model

Rotor performance calculations were performed using the comprehensive rotorcraft analysis CAMRAD II (Ref. 5). This model was previously used for performance correlation with WCB flight test data and has shown generally good results (Ref. 6). For the comparisons of analysis and test

data in this paper, the wide chord blade rotor was modeled as an isolated rotor. Nonlinear finite elements were used to model the elastic blades. The aerodynamic model included a free-wake analysis to calculate the rotor non-uniform induced-velocity field. This rotor wake analysis used second-order lifting line theory, with the general free wake geometry calculation. A dual-peak model was used for the performance calculations. Section lift, drag, and moment values from the SC2110 and SSCA09 airfoils were obtained from airfoil C81 decks developed by Sikorsky Aircraft.

The trim solution for forward flight solved for the controls to achieve the specified thrust level and zero 1/rev longitudinal and lateral flapping angles (± 0.01 deg).

Aircraft and Rotor Model

The UH-60 with wide chord blades was modeled as an aircraft with a single main and tail rotor in CAMRAD II. The trim solution is based on the aircraft gross weight, c.g., flight speed, rotor rpm, density, and outside air temperature and solves for the controls and aircraft attitudes that balance the forces and moment with zero sideslip angle. The horizontal stabilator angle was not acquired during the WCB/UH-60L flight test program and hence was unavailable as input for CAMRAD II. Instead the stabilator angle was based on the UH-60A Airloads Program measurements (Ref. 7) at a given C_W and μ. An aerodynamic interference model in CAMRAD II was used for the performance calculations. This includes the main rotor inflow interference effects on body, tail, and the tail rotor as time-averaged wake-induced velocity changes. No empirical factor was used for the calculation of the interference.

RESULTS AND DISCUSSION

The primary objective of the forward-flight wind tunnel testing was to acquire moderate to cruise speed performance data for comparison with and validation of analyses. To accomplish this objective, data were acquired over a range of advance ratios, shaft angles, and thrust levels (Table 4). In the sections below, these data are presented and compared with flight test data and CAMRAD II calculations.

All the wind tunnel performance results presented in Figs. 4-9,14-23 display normalized rotor power and rotor propulsive force coefficients. For ease of representation in these figures, the measured angles of the rotor shaft, α_S, are shown for thrust sweeps at various advance ratios. The actual corrected angle of attack values would increase in a positive direction relative to the physical shaft angle with increasing level of rotor lift.

Wind Tunnel Test Results

A representative set of 40 x 80 wind tunnel thrust sweep data is presented in Figs. 4-9; the full set is shown in Figs. 14-23. In general, the data show smooth trends and profiles similar to the standard UH-60 data acquired earlier (Ref. 8). These data will provide a valuable validation set for analytical development.

Figures 4-6 show the effect of rotor lift on rotor power at specific advance ratios and shaft angles. As expected, power increases with increasing lift and increasing forward shaft angle. The effect of advance ratio can be seen in the shape and spacing of the curves, with larger power differences between shaft angles at the higher advance ratios.

Figures 7-9 show the effect of rotor lift on propulsive force at specific advance ratios and shaft angles. For forward (negative) shaft angles the propulsive force increases linearly with increasing lift, whereas for zero shaft angle the propulsive force decreased.

Comparison between Wind Tunnel and Flight Test Data

To validate the wind tunnel test data, the data are compared with flight test data. Before the comparisons are performed, an assessment is made of the flight test data.

Assessment of Flight Test Data

Two sets of WCB level flight test data (1994 and 1999) were acquired with the same UH-60L aircraft at the same weight coefficient of 0.0065. The first flight test used the configuration 5 WCB set and the second flight test used the production WCB set. The flight test data presented are for two different c.g. conditions. Data from the 1994 test is for an aircraft “forward” c.g. of 348 in and data from the 1999 test is for an aircraft “mid” c.g. of 353 in. An assessment is made on the performance and pitch attitude of the two flight tests.

Figure 10 shows a comparison of total engine power for the two flight tests. The differences in aircraft c.g. and blades appear to have a negligible influence on the total aircraft power. Figure 11 shows the pitch attitude at various advance ratios for the two flight tests along with CAMRAD II predictions. Both data sets show a decrease in pitch attitude with increasing advance ratio. The pitch attitude for the forward c.g. (348 in) is approximately 3-4 deg more nose down compared to the mid c.g. configuration over the full speed range. Although the nose down pitch of the forward c.g. condition is expected, the 3-4 deg pitch attitude difference appears to be large for a 5 in c.g. difference. CAMRAD II calculations, based on aircraft and rotor

models, were performed to compare with the flight test data. CAMRAD II previously demonstrated good correlation with UH-60A aircraft pitch attitude, longitudinal flapping, and performance (Refs. 6 and 7). The present results from CAMRAD II compare well with the WCB flight test data at c.g. = 348 in (except at an advance ratio of 0.2). However, at a c.g. = 353 in, CAMRAD II does not compare well with the WCB flight test data. Because of the possibility of pitch attitude measurement errors and the lack of longitudinal flapping measurements, the flight test data could not be used in determining equivalent tip-path-plane angle settings for the rotor wind tunnel test conditions comparison study.

Comparison of Main Rotor Power between Wind Tunnel and Flight Test Data.

To help validate the 40 x 80 data, comparisons were made with data from the two WCB flight test programs. To match conditions between experiments, the predicted flight test tip-path-plane angle (calculated from CAMRAD II's prediction of pitch attitude and longitudinal flapping) and weight coefficient were used to interpolate the 40 x 80 data. It is assumed that $C_W = C_{LR}$ and shaft angle with wall corrections applied is equivalent to tip-path-plane angle. Figure 5 is an example of the 40 x 80 data used for interpolation, showing main rotor power as a function of lift for various rotor shaft angles for a constant advance ratio. In place of the physical shaft angle shown, the corrected rotor shaft angles would be used in the interpolation of the data.

Comparisons for two weight coefficients, $C_W = 0.0065$ and 0.0080, are shown in Figs. 12 and 13. In Fig. 12, speed sweep data from the flight test are compared with interpolated 40 x 80 data for $C_W = 0.0065$. The 40 x 80 data match well from an advance ratio of 0.15-0.30, but show a lower power requirement at the advance ratio of 0.35. Similar results can be seen in Fig. 13 for $C_W = 0.0080$. Possible causes for the differences include 40 x 80 measurement error, CAMRAD II accuracy of predicting pitch attitude and longitudinal flapping, flight test external conditions (wind direction, wind turbulence) in determining power, and flight test measurement errors (flight speed, aircraft attitude, flight control conditions).

Comparison with Predictions

To evaluate the capability of predicting moderate-to-cruise speed performance, CAMRAD II calculations were performed for all 40 x 80 thrust sweep conditions with wall corrections applied. The input data provided to CAMRAD II were the induced wall correction values for each C_{LR} and advance ratio condition which were required to perform power and propulsive force calculations.

Comparisons of CAMRAD II rotor power calculations with thrust sweep data are shown in Figs. 14-23 for five advance ratios (μ = 0.15, 0.20, 0.25, 0.30, and 0.35). Figure 14 shows rotor power as a function of lift at a fixed advance ratio of 0.15. CAMRAD II under predicts the 40 x 80 power data by varying levels depending on rotor lift and shaft angle. With increasing lift, under prediction increases at –10 and –5 degree shaft angles. At the shaft angle of 0 deg, CAMRAD II under predicts the 40 x 80 data throughout the lift range at a constant level. Some possible reasons for this under prediction are 1) the ability to accurately correct for wind tunnel wall effects at low speed and/or 2) ability in using CAMRAD II to set the proper wake modeling such as wake geometry, rotor tip wake roll up, or blade tip vortex size.

Figures 15 and 16 show rotor power as a function of lift at a fixed advance ratio of 0.20 and 0.25, respectively. CAMRAD II shows good correlation with the 40 x 80 power data at all rotor lift levels and shaft angles.

At an advance ratio of 0.30 (Fig. 17), calculated and measured power show similar agreement for all three shaft angles of –10 deg, –5 deg, and 0 deg. At a shaft angle of –10 deg, CAMRAD II slightly over predicts power at the low lift level and mid-lift level but under predicts at the higher lift levels. For shaft angles of –5 deg, CAMRAD II slightly over predicts power at the low lift level, matches at mid-lift level and under predicts at the higher lift levels. At 0 deg shaft angle, this trend continues. These same trends can be seen at the higher advance ratio of 0.35 (Fig. 18). The general result is that CAMRAD II slightly over predicts the required power at low lift levels and that this over prediction decreases with increasing lift at all shaft angles and advance ratios in most cases.

The effects of rotor shaft angle and thrust on rotor propulsive force for various advance ratios are shown in Figs. 19-23. For an advance ratio of 0.15, Fig. 19 shows CAMRAD II calculations match wind tunnel data at -10 and -5 deg shaft angle but slightly under predicts propulsive force at 0 deg shaft angle. At an advance ratio of 0.20, CAMRAD II calculation matches the measurements at all shaft angles (Fig. 20). At higher advance ratios, Figs. 21-23 show CAMRAD II calculations match at zero shaft angles but increasingly over predicts as shaft angle decreases and advance ratio increases.

These comparisons show that although CAMRAD II calculations provide good agreement with 40 x 80 power measurements and fair to good agreement with propulsive force measurements, additional improvements are needed at low speeds for power and at higher speeds for propulsive force.

CONCLUSIONS

A high-quality data set at forward speed was obtained to support future rotor developments and theory improvements. Performance results from the wide chord blade (WCB) rotor in the 40- by 80-Foot Wind Tunnel were compared with previous flight test data and calculations. The study resulted in the following conclusions:

1. The 40 x 80 forward-flight thrust sweep data show smooth trends.

2. The wind tunnel data match well with the WCB/UH-60L flight test at advance ratios from 0.15 to 0.30, but show lower power requirements at an advance ratio of 0.35.

3. Data from the two flight tests show that small aircraft c.g. shifts do not significantly affect overall rotor performance. The differences in measured pitch attitude are not understood. In order to perform comparison studies with flight test data, wind tunnel data, and predictions, it is important that accurate pitch attitude data and lateral/longitudinal blade flap data are acquired.

4. The analysis shows good correlation for main rotor power, but improvements are needed at low advance ratios. The general result is that CAMRAD II under predicts the required power at low lift levels, and this under prediction decreases with increasing lift and shaft angle at all advance ratios. CAMRAD II shows fair to good agreement with propulsive force.

ACKNOWLEDGEMENT

We would like to acknowledge the significant efforts of the WCB/LRTA test team in the conduct of this test program.

REFERENCES

1. Norman, T.R., Shinoda, P.M., Kitaplioglu, C., Jacklin, S.A., and Sheikman, A., "Low-Speed Wind Tunnel Investigation of a Full-Scale UH-60 Rotor System," American Helicopter Society 58th Annual Forum, Montreal, Canada, June 2002.

2. Van Aken, J. M., Shinoda, P. M., and Haddad, F., "Development of a Calibration Rig for a Large Multi-Component Rotor Balance," 46th International Instrumentation Symposium of the Instrument Society of America, Bellevue, WA, May 2000.

3. Glauert, H., "The Interference on the Characteristics of an Airfoil in a Wind Tunnel of Rectangular Section," R & M 1459, 1932.

4. Johnson, W. and Silva, F., "Rotor Data Reduction System User's Manual for the National Full-Scale Aerodynamics Complex NASA Ames Research Center," 1986.

5. Johnson, W., "Rotorcraft Aerodynamics Model for a Comprehensive Analysis," American Helicopter Society 54th Annual Forum, Washington, D.C., May 1998.

6. Yeo, H., Bousman, W.G., and Johnson, W., "Performance Analysis of a Utility Helicopter with Standard and Advanced Rotors," American Helicopter Society Aerodynamics, Acoustics, and Test and Evaluation Technical Specialists Meeting, San Francisco, CA, January 2002.

7. Kufeld, R. M., Balough, D. L., Cross, J. L., Studebaker, K. L., Jennison, C. D., and Bousman, W. G., "Flight Testing the UH-60A Airloads Aircraft," American Helicopter Society 50th Annual Forum, Washington D.C., May 1994.

8. Shinoda, P.M., Yeo, H., and Norman, T.R., "Rotor Performance of a UH-60 Rotor System in the NASA Ames 80- by 120-Foot Wind Tunnel," American Helicopter Society 58th Annual Forum, Montreal, Canada, June 2002.

Table 1. UH-60 Main Rotor Parameters

Parameter	Wide Chord Blades (WCB)	Standard UH-60 Blades
Number of Blades	4	4
Radius	26.83 ft	26.83 ft
Nominal Chord	24.25 in	20.76 in
Rotor Disk Area	2261.5 ft^2	2261.5 ft^2
Rotor Blade Area	205.6 ft^2	186.9 ft^2
Solidity Ratio	.0909	.0826
Airfoils	SC2110/ SSCA09	SC1095/ SC1094 R8 SC1095
Nominal Rotor Speed	258 rpm	258 rpm
Nominal Tip Speed	725 ft/sec	725 ft/sec

Table 2. Rotor Balance Capabilities

Parameter	Maximum Capacity		Unsteady 1/2 Peak-to Peak
	Min	Max	
Thrust	-3,000 lb	52,000 lb	12,000 lb
Hub Force	-15,000 lb	15,000 lb	5,000 lb
Hub Moment	-50,000 ft-lb	50,000 ft-lb	21,000 ft-lb
Torque	0 ft-lb	164,800 ft-lb	7,800 ft-lb

Table 3. LRTA Balance Accuracy

Parameter	Maximum Cal. Load	Estimated Uncertainty	
		Value	%
Normal Force	30,000 lb	60 lb	0.20
Axial Force	15,000 lb	20 lb	0.13
Side Force	15,000 lb	20 lb	0.13
Pitch Moment	83,000 ft-lb	100 ft-lb	0.12
Roll Moment	83,000 ft-lb	200 ft-lb	0.24

Table 4. Thrust Sweep Test Matrix

Advance Ratio μ	Rotor Shaft Angle-of-Attack α_s	Approx. C_T Range
0.150	-10°, -5°, 0°	.004 - .009
0.200	-10°, -5°, 0°	.004 - .009
0.250	-10°, -5°, 0°	.004 - .009
0.300	-10°, -5° ,0°	.004 - .009
0.350	-10°, -5°	.004 - .009

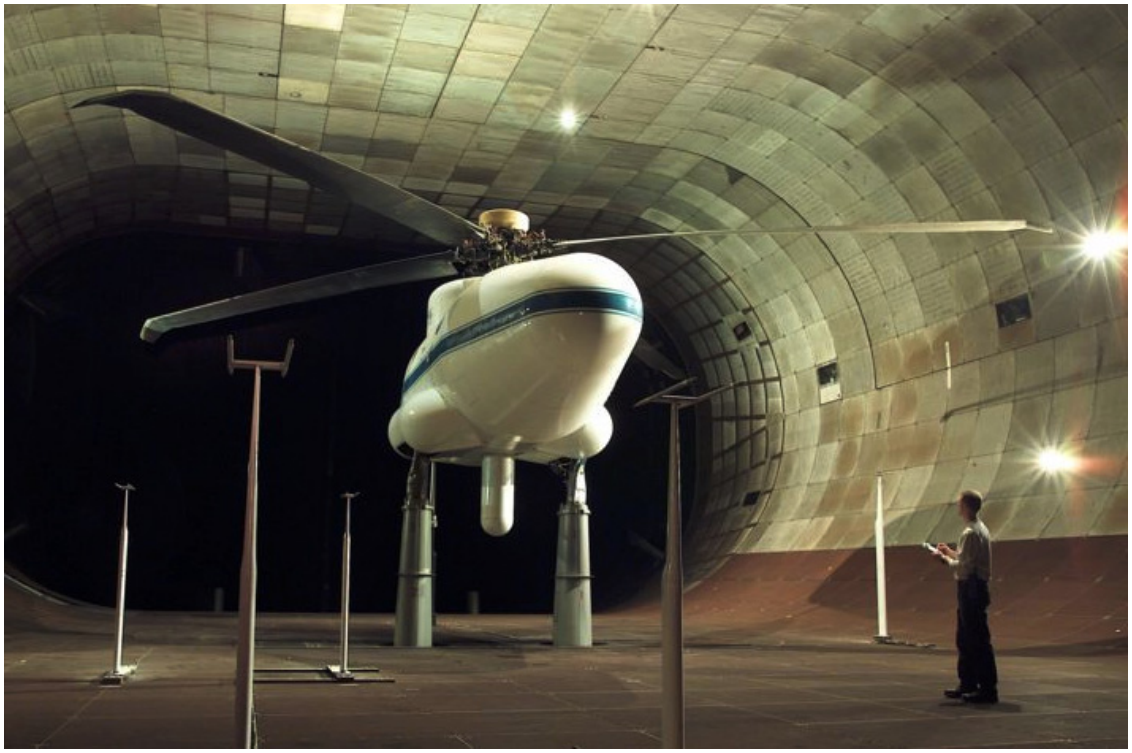

Fig. 1 Wide Chord Blade/UH-60 Rotor System installed on Large Rotor Test Apparatus in the Ames 40- by 80-Foot Wind Tunnel.

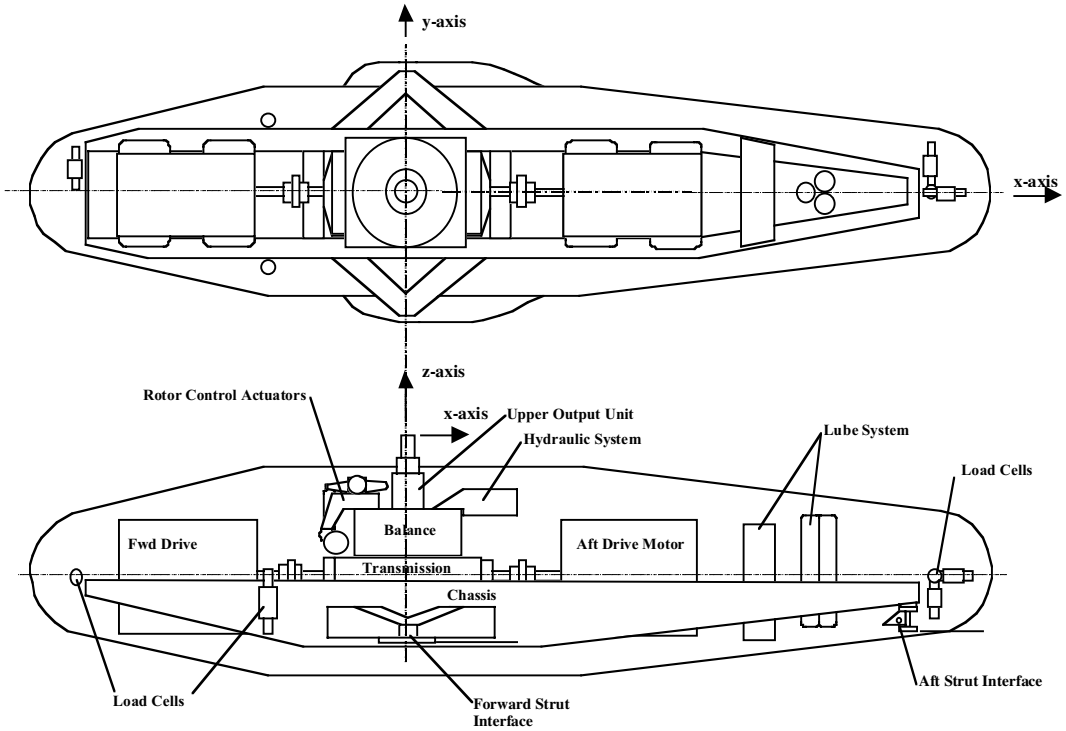

Fig. 2 Schematic of the Large Rotor Test Apparatus.

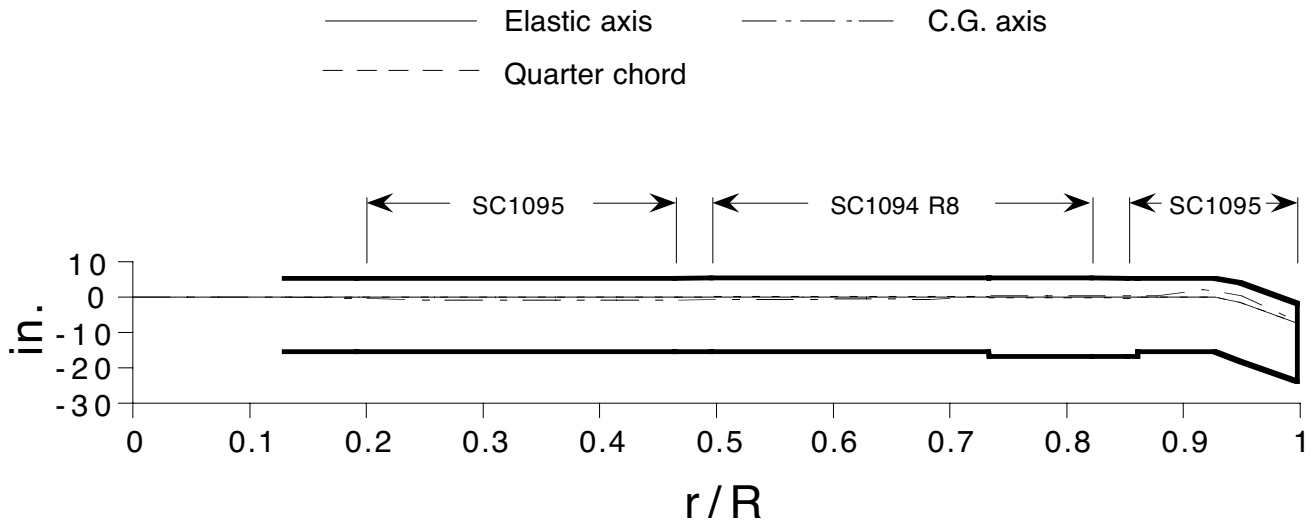

(a) Standard blade

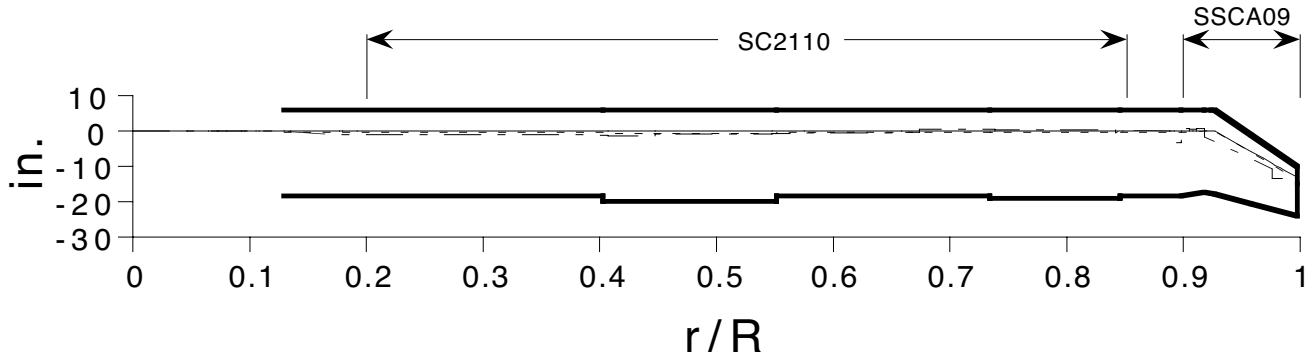

(b) Wide chord blade

Fig. 3 UH-60 Black Hawk rotor blade planforms.

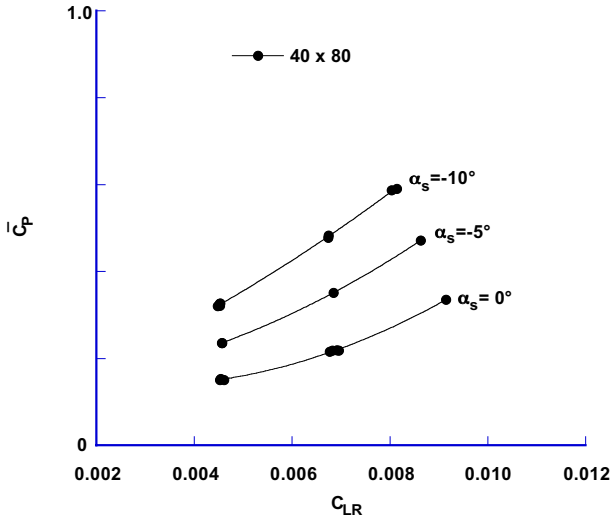

Fig. 4 Measured 40 x 80 WCB main rotor power vs. rotor lift for various rotor shaft angles at an advance ratio of 0.200.

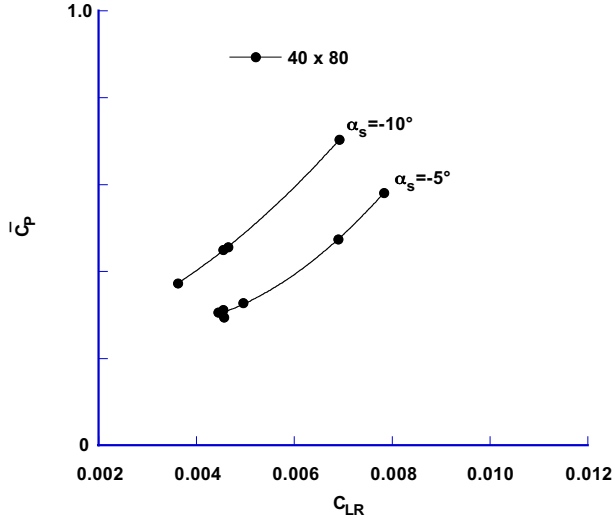

Fig. 6 Measured 40 x 80 WCB main rotor power vs. rotor lift for various rotor shaft angles at an advance ratio of 0.350.

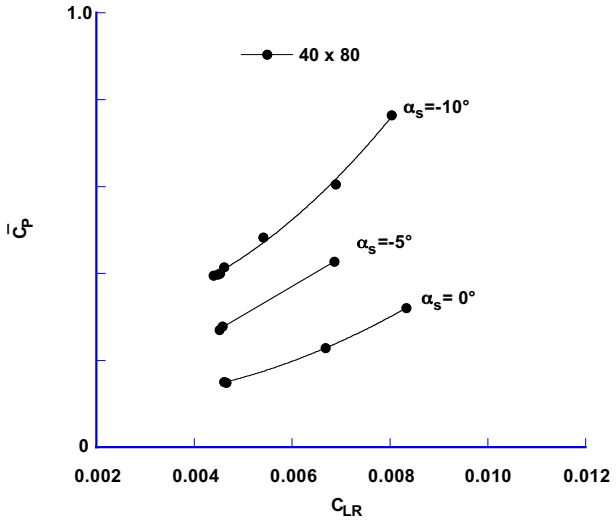

Fig. 5 Measured 40 x 80 WCB main rotor power vs. rotor lift for various rotor shaft angles at an advance ratio of 0.300.

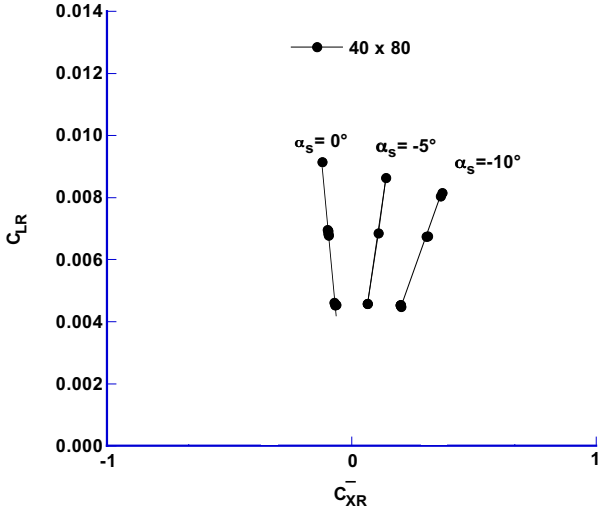

Fig. 7 Measured 40 x 80 WCB rotor lift vs. rotor propulsive force for various rotor shaft angles at an advance ratio of 0.200.

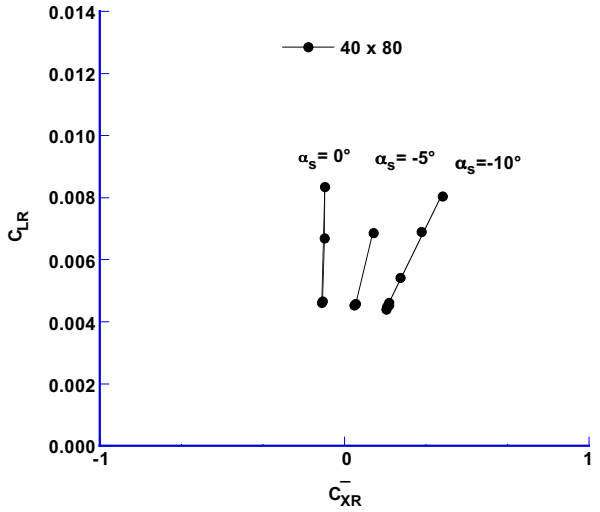

Fig. 8 Measured 40 x 80 WCB rotor lift vs. rotor propulsive force for various rotor shaft angles at an advance ratio of 0.300.

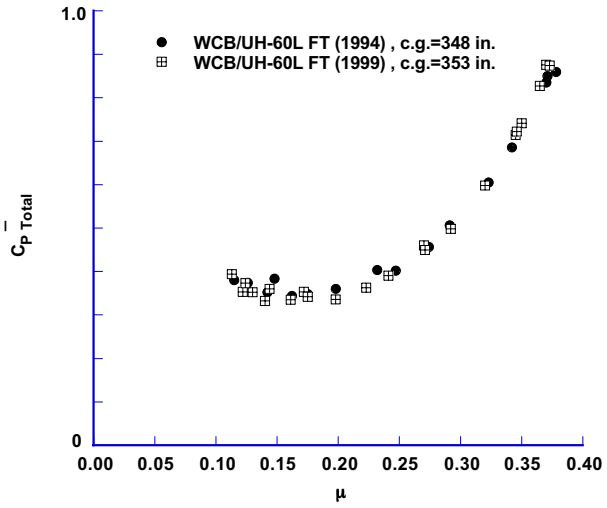

Fig. 10 Measured total engine power vs. advance ratio for two WCB/UH-60L test programs, $C_W = 0.0065$.

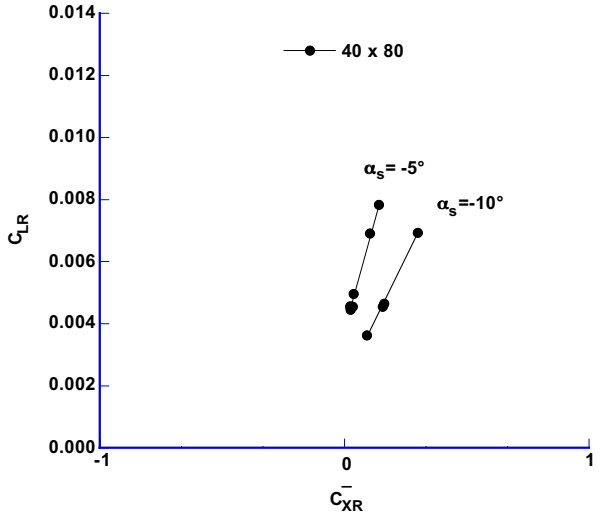

Fig. 9 Measured 40 x 80 WCB rotor lift vs. rotor propulsive force for various rotor shaft angles at an advance ratio of 0.350.

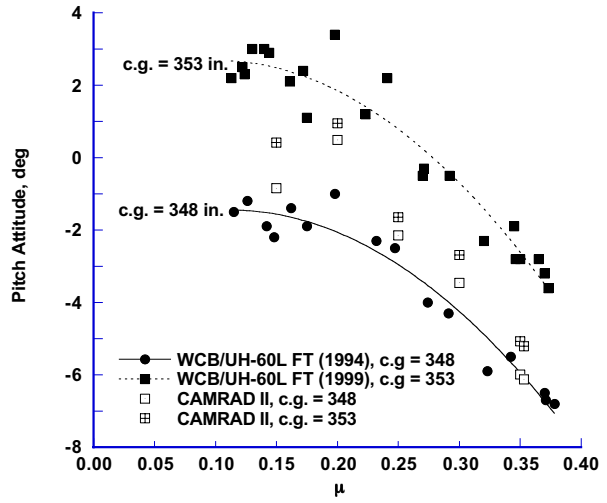

Fig. 11 Measured and calculated aircraft pitch attitude vs. advance ratio, $C_W = 0.0065$.

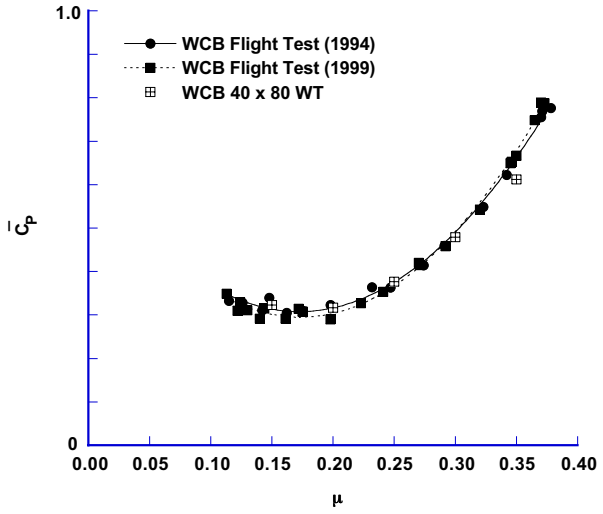

Fig. 12 WCB flight test and 40 x 80 measured main rotor power vs. advance ratio, $C_W = 0.0065$.

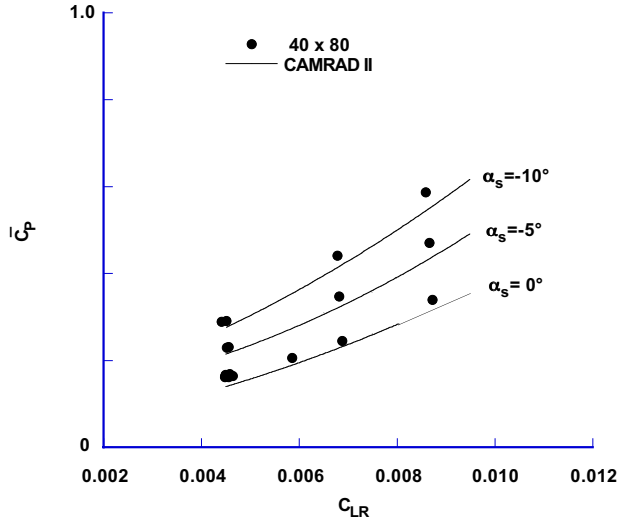

Fig. 14 Measured and calculated WCB main rotor power vs. rotor lift for various rotor shaft angles at an advance ratio of 0.150.

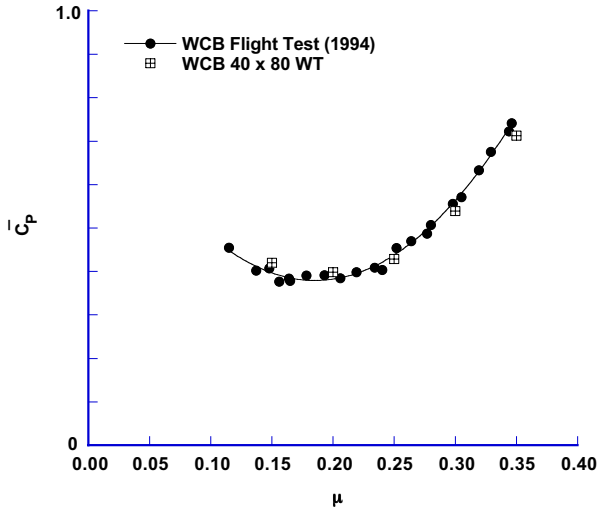

Fig. 13 WCB flight test and 40 x 80 measured main rotor power vs. advance ratio, $C_W = 0.0080$.

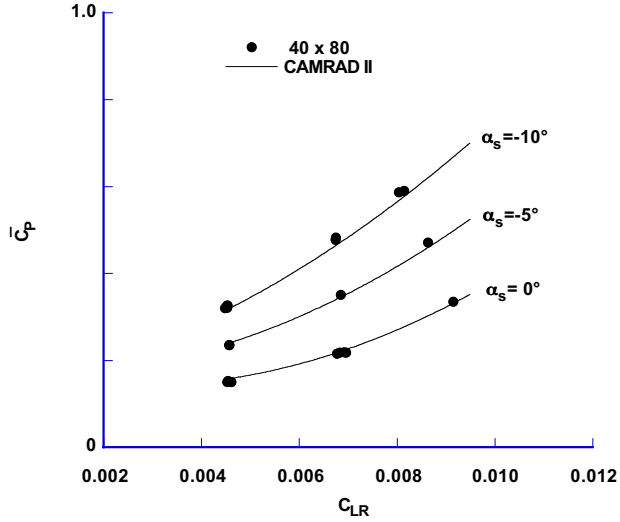

Fig. 15 Measured and calculated WCB main rotor power vs. rotor lift for various rotor shaft angles at an advance ratio of 0.200.

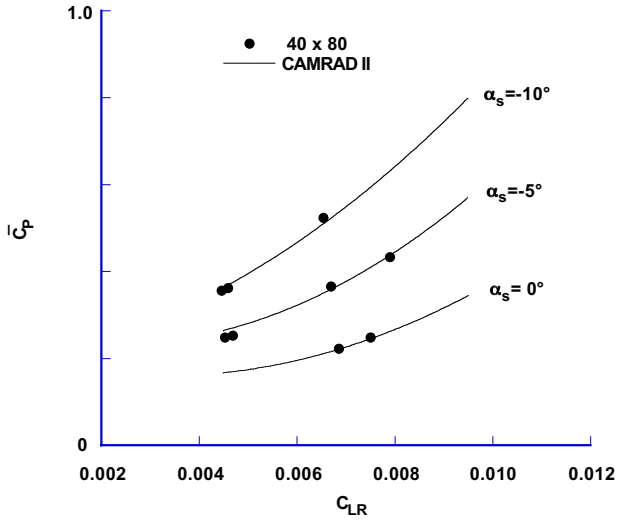

Fig. 16 Measured and calculated WCB main rotor power vs. rotor lift for various rotor shaft angles at an advance ratio of 0.250.

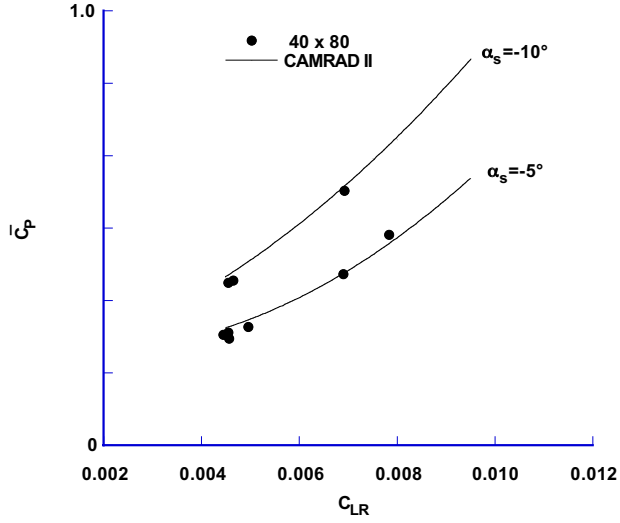

Fig. 18 Measured and calculated WCB main rotor power vs. rotor lift for various rotor shaft angles at an advance ratio of 0.350.

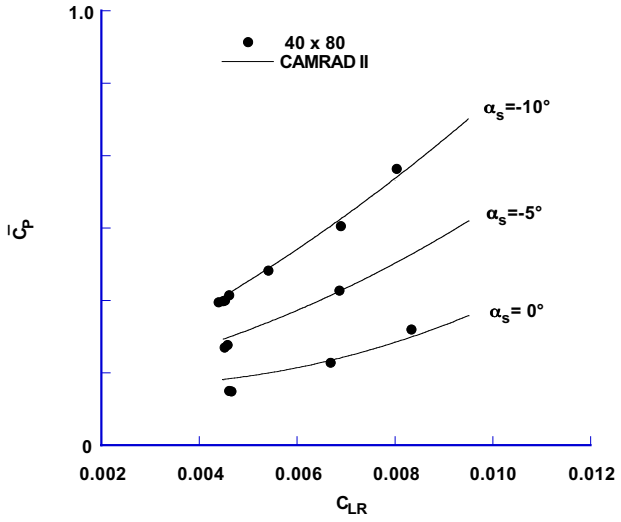

Fig. 17 Measured and calculated WCB main rotor power vs. rotor lift for various rotor shaft angles at an advance ratio of 0.300.

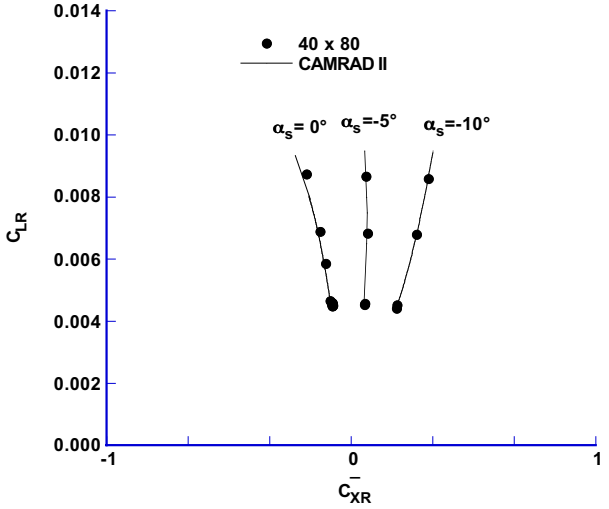

Fig. 19 Measured and calculated WCB rotor lift vs. rotor propulsive force for various rotor shaft angles at an advance ratio of 0.150.

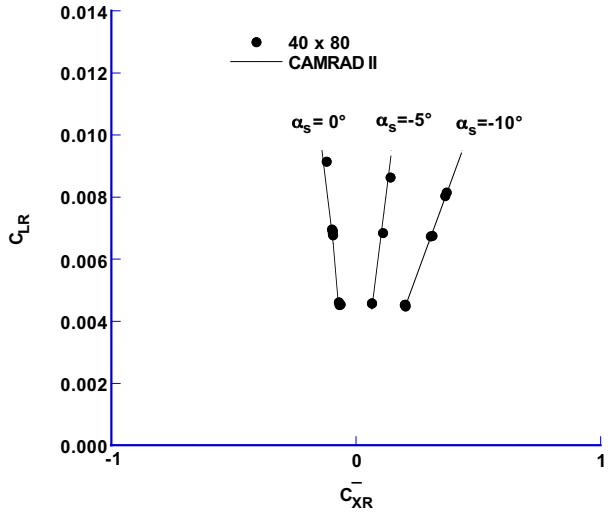

Fig. 20 Measured and calculated WCB rotor lift vs. rotor propulsive force for various rotor shaft angles at an advance ratio of 0.200.

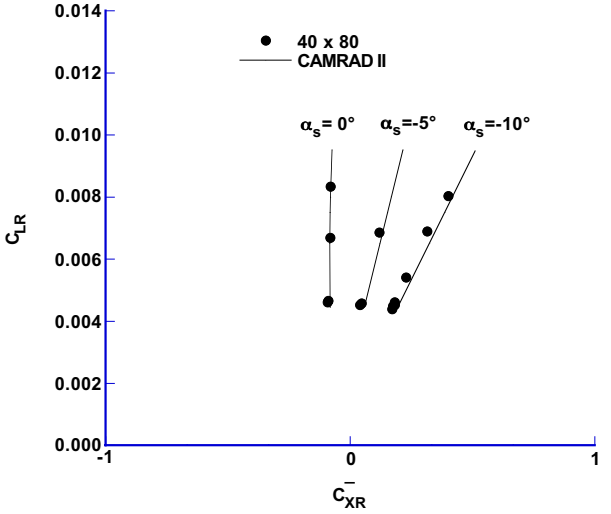

Fig. 22 Measured and calculated WCB rotor lift vs. rotor propulsive force for various rotor shaft angles at an advance ratio of 0.300.

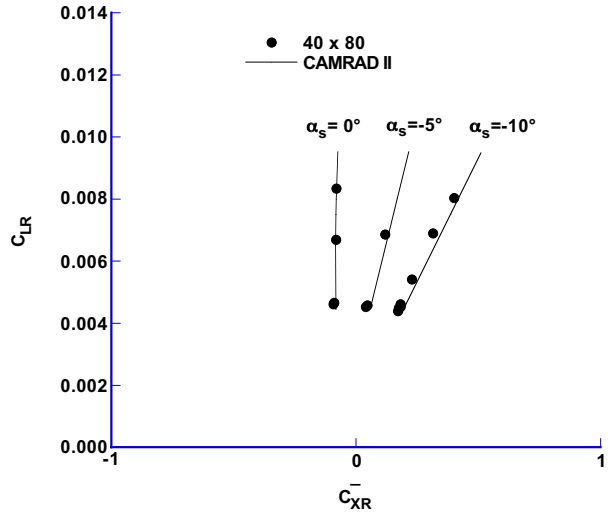

Fig. 21 Measured and calculated WCB rotor lift vs. rotor propulsive force for various rotor shaft angles at an advance ratio of 0.250.

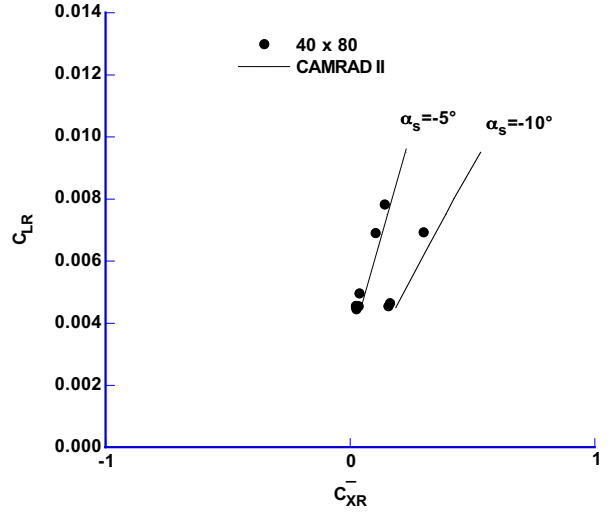

Fig. 23 Measured and calculated WCB rotor lift vs. rotor propulsive force for various rotor shaft angles at an advance ratio of 0.350.